

New Metallic Carbon Crystal

Masahiro Itoh

Institute of Multidisciplinary Research for Advanced Materials, Tohoku University, Aoba-ku, Sendai 980-8577, Japan

Motoko Kotani

Mathematical Institute, Graduate School of Science, Tohoku University, Aoba-ku, Sendai 980-8578, Japan

Hisashi Naito

Graduate School of Mathematics, Nagoya University, Chikusa-ku, Nagoya 464-8602, Japan

Toshikazu Sunada

Department of Mathematics, Meiji University, Tama-ku, Kawasaki 214-8571, Japan

Yoshiyuki Kawazoe

Institute for Materials Research, Tohoku University, Aoba-ku, Sendai 980-8577, Japan

Tadafumi Adschiri*

*Institute for Materials Research, Tohoku University, Aoba-ku, Sendai 980-8577, Japan,
and Advanced Institute for Materials Research, WPI, Tohoku University, Aoba-ku, Sendai 980-8577, Japan*
(Received 12 June 2008; published 4 February 2009)

Recently, mathematical analysis clarified that sp^2 hybridized carbon should have a three-dimensional crystal structure (K_4) which can be regarded as a twin of the sp^3 diamond crystal. In this study, various physical properties of the K_4 carbon crystal, especially for the electronic properties, were evaluated by first principles calculations. Although the K_4 crystal is in a metastable state, a possible pressure induced structural phase transition from graphite to K_4 was suggested. Twisted π states across the Fermi level result in metallic properties in a new carbon crystal.

DOI: 10.1103/PhysRevLett.102.055703

PACS numbers: 64.60.My, 61.66.Bi, 64.70.K-, 71.15.Mb

Carbon has been known to have only three structures: diamond, graphite, and amorphous. About 40 years ago, diamondlike carbon was defined in a study on chemical vapor deposition [1]. There are also recent reports on other carbon structures including fullerene [2,3], carbon nanotubes [4], and others [5–13]. However, the diamond structure that has sp^3 hybrid states is widely accepted as the only three-dimensional crystal structure of carbon. Very recently, mathematical analysis [14] clarified that sp^2 bonded systems should have another attractive 3D structure (K_4 crystal).

The electronic property of carbon is one of the most important properties for its applications, such as solid-state devices and electrodes. Diamond is a well-known insulator [15], and a graphene sheet shows various properties depending on its structure (e.g., single-layer graphene, and arm-chair, zig-zag and chiral carbon nanotubes) [16,17]. For the case of fullerene, and carbon nanotubes, the electronic property changes drastically by doping a metallic element [18,19]. For the K_4 crystal, the electronic property has not been discussed yet.

In this Letter, it is demonstrated for the first time that the new carbon, K_4 , exhibits metallic properties. Also, the stability of K_4 and possible phase transition from graphite to K_4 is discussed with the suggested existence of this new carbon.

In this study, first principles calculations based on density functional theory [20,21] were performed for diamond, graphite, and K_4 crystals by employing the Vienna *ab initio* simulation package (VASP) [22]. Local density approximation (LDA) [23,24] and generalized gradient approximation (GGA) developed by Perdew and Wang [25] were used for the exchange-correlation energy functional. In these calculations, all three crystals were regarded as spin-unpolarized systems. For reducing the computational costs, a projector-augmented wave method [26] was employed to approximate a nucleus, inner core electrons, and valence electrons in each atom of the crystal. For a carbon atom, $2s^2 2p^2$ electrons were considered as the valence electrons.

For the total energy calculation, each unit cell of the crystal was selected, as shown in the inset of Fig. 1(b). The space groups of diamond, graphite, and K_4 crystals are $Fd\bar{3}m (O_h^7)$, $P6_3/mmc (D_{6h}^4)$, and $I4_132 (O^8)$, respectively.

For the crystals, V_0 (volume V at lattice constant), d_0 (nearest-neighbor distance), E_{coh} (cohesive energy), and B_0 (bulk modulus at V_0) were determined by evaluating the total energy of the hypothesized crystal structure. B_0 can be a criterion of hardness of a bulk crystal [15]. Murnaghan's equation of state [27] was used as a fitting curve to the calculated values of total energy vs volume. Parameters in the equation were determined using the least squares method in the range of $0.8V_0 < V < 1.2V_0$,

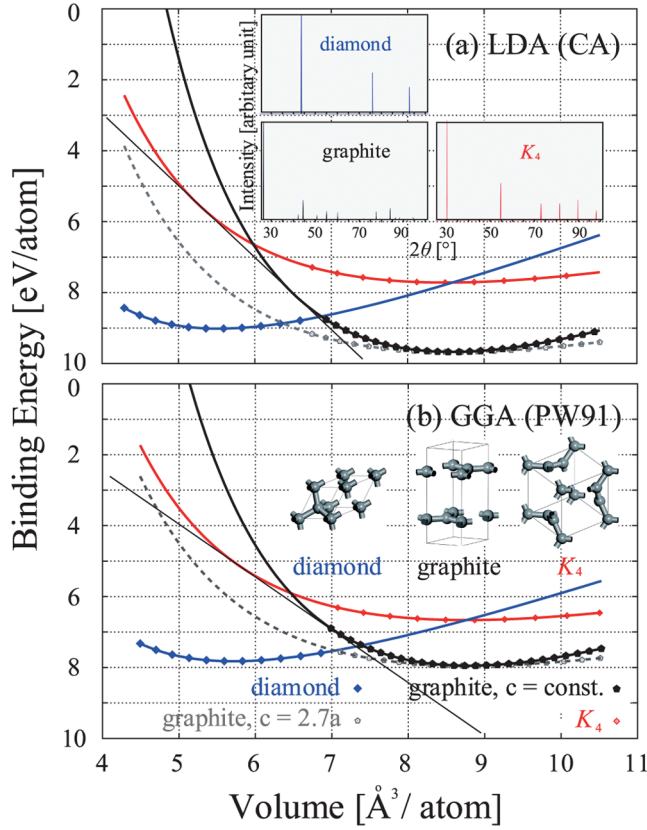


FIG. 1 (color). Binding energy vs volume curves of diamond (blue), graphite (grey and black), and K_4 (red) crystal structures composed of carbon atoms based on (a) LDA, and (b) GGA developed by Ceparley and Alder (CA) [24], and Perdew and Wang (PW91) [25]; The curves are fits of the Murnaghan's equation of state [27] to the calculated points. Tangential line between the curves of K_4 -graphite crystals; XRD patterns [in the inset of (a)].

where the root mean square was set to be less than 1.5 meV/atom.

The cutoff energy for the plane-wave expansion of valence electrons was changed, so that the number of plane waves are constant over a full range of lattice constant. Around the minimum of the binding energy vs volume curve, the values were set to be 500 eV for each crystal. The calculation results are the same, even if we set the values as 1000 eV.

Brillouin zone integration was performed for k -point meshes generated by the Monkhorst-Pack scheme. For diamond, graphite, and K_4 crystals, $10 \times 10 \times 10$, $8 \times 8 \times 4$, and $8 \times 8 \times 8$ meshes, respectively, were selected. The residual minimization direct inversion in the iterative subspace (RMM-DIIS) method is used to accelerate the convergence of self-consistent total energy calculations. The convergence criterion was set to be within 5.0×10^{-6} eV/atom.

Figure 1 lists the total energy vs volume curves for diamond, graphite, and K_4 , and Table I shows various physical properties such as V_0 , d_0 , E_{coh} , and B_0 determined from the

curves. In this table, previously reported results of first principles calculations and experiments for diamond and graphite are also listed for comparison. Our calculations are in relatively good agreement with previously reported first principles calculations and the experimental results that suggest the validity of LDA and GGA of this study.

As expected, V_0 is the largest and B_0 is the smallest for K_4 for the isotropic change in V . For the relationship between E_{coh} and d_0 , although E_{coh} of K_4 is the smallest, d_0 of K_4 is still shorter than that of diamond. These specific physical properties are discussed later, based on the electronic states.

For the K_4 crystal, Hellman-Feynman forces acting on each atom were also evaluated to confirm the structural stability around volume $V = V_0$. For both LDA and GGA, the K_4 crystal structure shows the stability around $V = V_0$. Here, it is essential that the K_4 crystal shows structural stability on the potential energy surface, although it is in a metastable state.

A possibility of pressure-induced structural phase transition between different crystal structures was investigated to confirm whether the K_4 crystal is produced or not, by using a thermodynamic phase transition theory [33]. According to this theory, a negative slope of the tangent line between the energy vs volume curves of two different crystals indicates the positive transition pressure P_t which allows pressure-induced structural phase transition between them.

To the K_4 crystal, it is apparent that P_t takes positive value only from a graphite crystal with a pressure induction parallel to the a axis. Here, $P_{t, \text{graphite}-K_4}$ is 3.19×10^{11} [N/m²] in LDA, and 2.39×10^{11} [N/m²] in GGA, which are almost 1 order of magnitude higher than $P_{t, \text{graphite}-\text{diamond}}$. These results suggest that the K_4 crystal can be formed from graphite, but diamond seems to be formed more preferably by the pressure-induced structural phase transition. However, if the pressure is rapidly elevated to $P_{t, \text{graphite}-K_4}$ at a faster rate than the rate of crystal transformation from graphite to diamond, the K_4 crystal can be formed.

The inset of Fig. 1(a) shows x-ray diffraction (XRD) patterns of a K_4 crystal at volume V_0 evaluated by our LDA calculations. Monochromatic radiation with a wavelength 1.541 Å is assumed in this calculation. XRD patterns of diamond and graphite are also shown for comparison. The relative positions, and intensities of the peaks show relatively good agreement with the experimental values for diamond and graphite [28]. As shown in this figure, K_4 has a specific XRD peak at $2\theta = 31^\circ$.

The LDA and GGA calculations show the same results qualitatively. Thus, for the following discussion, LDA calculation results were employed.

Figures 2(a) and 2(b), show the electronic density of states and band structures in the diamond, graphite, and K_4 crystals. As is widely known, diamond and graphite show properties of insulators [15] and semimetals [15,29,30], respectively. Surprisingly, the K_4 crystal shows a metallic

TABLE I. Both theoretically and experimentally evaluated structural parameters for the diamond, graphite and K_4 crystal. Determined V_0 (volume V at lattice constant), d_0 (nearest neighbor distance), E_{coh} (cohesive energy), and B_0 (bulk modulus at V_0) are shown. LDA and GGA mean approximation in exchange-correlation functional in each calculation based on the density functional theory. PW91 corresponds to the expression for the approximation developed by Perdew and Wang [25]. For graphite crystal, (1) a and c were varied with keeping $c/a = 2.7$, which is expected at 0 K from experimental results [28–32], (2) a was varied at $c = \text{constant}$ [minimum value of case (1)].

Structure	Method	Source	$V_0[\text{\AA}^3/\text{atom}]$	$d_0[\text{\AA}]$	$E_{\text{coh}}[\text{eV}/\text{atom}]$	$B_0[10^{11} \frac{\text{N}}{\text{m}^2}]$
Diamond	GGA (PW91)	This Letter	5.709	1.548	7.831	4.24
Diamond	LDA	This Letter	5.524	1.531	9.000	4.58
Diamond	LDA	[30]	5.498	1.529	9.004	4.60
Diamond	Expt.	[15]	5.67	1.54	7.37	4.43
Graphite ($c = 2.7a$)	GGA (PW91)	This Letter	8.811	1.424	7.957	2.71
Graphite ($c = 6.670 \text{\AA}$)	GGA (PW91)	This Letter	8.789	1.424	7.956	6.08
Graphite ($c = 2.7a$)	LDA	This Letter	8.606	1.413	9.659	2.80
Graphite ($c = 6.618 \text{\AA}$)	LDA	This Letter	8.581	1.413	9.658	6.28
Graphite ($c = 2.734a$)	LDA	[30]	8.627	1.410	9.001	2.88
Graphite ($c = 2.7a - 2.73a$)	Expt.	[30]	8.734–8.797	1.420	7.374	2.86–3.19
K_4	GGA (PW91)	This Letter	8.763	1.458	6.670	2.49
K_4	LDA	This Letter	8.502	1.443	7.702	2.67

feature, as the band gap around the Fermi level could not be observed. High degeneracy in the density of states is a specific feature of K_4 . For K_4 , the p character is significant near the highest occupied molecular orbital state, which results in metallic properties. The electronic states forming partial valence-electron density were classified from their spatial density distributions and the number of states characterized by s and/or p orbital for each primitive unit cell are shown in the right-hand side of Fig. 2(c).

Figures 2(c) and 2(d), show the isosurfaces of the partial and total valence-electron density in the diamond, graphite, and K_4 crystals. The isosurface ($1.5e/\text{\AA}^3$) of the charge density of total valence electrons for diamond, graphite, and K_4 , which is shown in Fig. 2(d), clearly demonstrates that valence electrons are distributed around the bonds between nearest neighbor atoms. A clear difference between diamond and the other two crystals in the middle

part of the bonds can be observed. In the diamond crystal, the isosurface is shrunken in the middle part in contrast with the graphite, and K_4 crystals. These differences are explained below.

In the case of diamond, for lower energy levels, $2s-2s$ type bonds appear predominantly. However, for higher energy levels, the p character becomes stronger, and as a result, $2s2p^3-2s2p^3$ type bonds appear predominantly. The shrinkage in the middle part of each bond shown in Fig. 2(d) originates from these features. In the case of graphite, for lower energy levels, the $2s-2s$ type bonds appear predominantly, and when the energy of states is higher, the p character becomes stronger, similar to the case of diamond. However, different from the case of diamond, when the energy level is higher, $2s2p^2-2s2p^2$ and $2p-2p$ (π) type bonds appear explicitly. In this case, the shrinkage in the electron density around the middle part

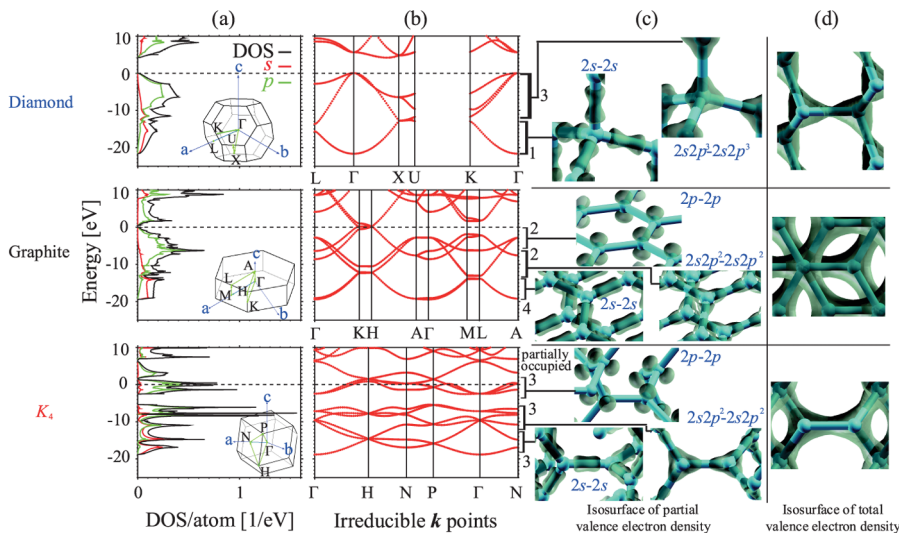


FIG. 2 (color). (a) Total and partial density of states (DOS). (b) Band structures for the valence electrons based on LDA calculations. The first Brillouin zone with selected pass for the electronic band structure [in the inset of (a)]. (c) The partial valence-electron density. The number of partial valence-electron densities for each group in a primitive unit cell [right side of (b)]. (d) Isosurfaces of the total valence-electron density.

of the bonds cannot be found, which is probably due to the more uniform $2s$ - $2s$ type electron density along the bonds, as shown in Fig. 2(c). The electronic state of K_4 is nearly the same as that of graphite. However, twisted $2p$ - $2p$ (incomplete π) type bonds are formed. The metallic property of K_4 can be attributed to the raising of these $2p$ -type states to energy levels higher than the Fermi level. From those results, the difference in d_0 , E_{coh} , B_0 and V_0 can be explained.

As mentioned earlier, graphite and K_4 have smaller d_0 than diamond, whereas K_4 has smaller E_{coh} than diamond and graphite. The common feature of graphite and K_4 that distinguishes them from diamond is the existence of $2s2p^2$ - $2s2p^2$ and $2p$ - $2p$ type bonds. The large difference in E_{coh} between graphite and K_4 originates from the completeness of the π -type bonds. Here, because bond strength depends on d_0 , the cohesive energy per unit bond ($E_{\text{coh}}/(\text{number of bonds per atom}) \equiv e$) should be discussed: $e_{\text{graphite}} = 3.320$, $e_{K_4} = 2.567$, and $e_{\text{diamond}} = 2.250$ eV. Both the bond strength e and the nearest-neighbor atomic distance d_0 , can be characterized by the bond types (sp^2 , or sp^3 , and the existence of π). As discussed above, the valence-electron density along a bond for K_4 and graphite is higher than that for diamond ($\text{diamond}(d) < K_4 \leq \text{graphite}(g)$), which is attributed to the shorter d_0 ($d > K_4 \geq g$) and larger e ($d < K_4 < g$). The completeness of π bonds also attribute to the difference between e_{graphite} and e_{K_4} .

One of the reasons for this is the difference in volume change resulting from the bond length change which originates from the difference in the manner of compression and the atomic density. Namely, to make the same degree of change in the bond length, a larger volume change is needed in the K_4 crystal and this contributes to the large difference in B_0 between K_4 and graphite with compression parallel to the a axis. Further, the interaction of electrons along the bonds should be considered. Namely, in contrast to graphite, in the K_4 crystal, the twisted π states along each bond are expected to weaken the orbital-orbital interactions and allow the geometric change. In the case of diamond, $2s2p^3$ type electrons interact strongly with each other; therefore, it has extremely high B_0 (low compressibility). The difference in V_0 originates from the difference in the chemical bonds and inherent crystal structures.

This study focused on the metallic behavior and the possible existence of K_4 . However, because the K_4 crystal can be considered as a chiral web of decagonal rings of sp^2 hybridized carbon atoms, a comparison with the interplay of chirality and metallic/semiconducting properties of carbon nanotubes could be interesting. A comparative discussion of the metallic behavior from this viewpoint will be presented elsewhere.

The authors acknowledge the staff of the CCMS, IMR for allowing the use of the HITACHI SR11000 supercomputing facilities. We acknowledge financial support from

the MEXT, WPI and CREST. We acknowledge Dr Anton Kokalj for the use of the visualization program XCRYSDEN [34] for the visualization in Fig. 2.

*ajiri@tagen.tohoku.ac.jp

- [1] S. Aisenberg and R. Chabot, J. Appl. Phys. **42**, 2953 (1971).
- [2] H. W. Kroto *et al.*, Nature (London) **318**, 162 (1985).
- [3] E. Ohsawa, Kagaku **25**, 850 (1970).
- [4] S. Iijima, Nature (London) **354**, 56 (1991).
- [5] M. T. Yin, Phys. Rev. B **30**, 1773 (1984).
- [6] A. Y. Liu and M. L. Cohen, Phys. Rev. B **45**, 4579 (1992), and references therein.
- [7] M. C. Jeffrey *et al.*, Phys. Rev. B **58**, 664 (1998).
- [8] F. J. Ribeiro *et al.*, Phys. Rev. B **74**, 172101 (2006), and references therein.
- [9] A. E. Goresy *et al.*, Comput. Geosci. **335**, 889 (2003).
- [10] A. F. Wells, Acta Crystallogr. **7**, 535 (1954).
- [11] M. O'Keeffe, G. B. Adams, and O. Sankery, Phys. Rev. Lett. **68**, 2325 (1992).
- [12] B. Winkler *et al.*, Chem. Phys. Lett. **337**, 36 (2001).
- [13] R. T. Strong *et al.*, Phys. Rev. B **70**, 045101 (2004), and references therein.
- [14] T. Sunada, Not. Am. Math. Soc. **55**, 208 (2008).
- [15] C. Kittel, *Introduction to Solid State Physics* (John Wiley & Sons, Inc., New York, 1996).
- [16] N. Hamada, S. Sawada, and A. Oshiyama, Phys. Rev. Lett. **68**, 1579 (1992).
- [17] K. Sasaki *et al.*, Phys. Rev. B **71**, 195401 (2005).
- [18] *Clusters and Nanomaterials*, edited by Y. Kawazoe, T. Kondow, and K. Ohno (Springer, New York, 2002), and references therein.
- [19] Y. Yagi *et al.*, Phys. Rev. B **69**, 075414 (2004), and references therein.
- [20] P. Hohenberg and W. Kohn, Phys. Rev. **136**, B864 (1964).
- [21] W. Kohn and L. J. Sham, Phys. Rev. **140**, A1133 (1965).
- [22] G. Kresse and J. Furthmüller, Phys. Rev. B **54**, 11 169 (1996).
- [23] J. P. Perdew and A. Zunger, Phys. Rev. B **23**, 5048 (1981).
- [24] D. M. Ceperley and B. J. Alder, Phys. Rev. Lett. **45**, 566 (1980).
- [25] J. P. Perdew *et al.*, Phys. Rev. B **46**, 6671 (1992).
- [26] P. E. Blöchl, Phys. Rev. B **50**, 17 953 (1994).
- [27] F. D. Murnaghan, Proc. Natl. Acad. Sci. U.S.A. **30**, 244 (1944).
- [28] O. O. Mykhaylyk *et al.*, J. Appl. Phys. **97**, 074302 (2005).
- [29] J. C. Boettger, Phys. Rev. B **55**, 11 202 (1997), and references therein.
- [30] J. Furthmüller, J. Hafner, and G. Kresse, Phys. Rev. B **50**, 15 606 (1994), and references therein.
- [31] Von A. Ludsteck, Acta Crystallogr. Sect. A **28**, 59 (1972).
- [32] H. J. F. Jansen and A. J. Freeman, Phys. Rev. B **35**, 8207 (1987).
- [33] J. Hafner, *From Hamiltonians to Phase Diagrams, The Electronic and Statistical-Mechanical Theory of sp-Bonded Metals and Alloys*, Springer Ser. Solid-State Sci. Vol. 70 (Springer-Verlag, Berlin, 1987).
- [34] A. Kokalj, Comput. Mater. Sci. **28**, 155 (2003).